



PERGAMON

Available online at [www.sciencedirect.com](http://www.sciencedirect.com)

SCIENCE @ DIRECT®

Continental Shelf Research 23 (2003) 901–918

CONTINENTAL SHELF  
RESEARCH

[www.elsevier.com/locate/csr](http://www.elsevier.com/locate/csr)

# Long-term, high-frequency current and temperature measurements along central California: insights into upwelling/relaxation and internal waves on the inner shelf

C.D. Storlazzi<sup>a,\*</sup>, M.A. McManus<sup>b</sup>, J.D. Figurski<sup>b</sup>

<sup>a</sup> US Geological Survey, Pacific Science Center, 1156 High Street, Santa Cruz, CA 95064-1077, USA

<sup>b</sup> Institute of Marine Sciences, University of California, 1156 High Street, Santa Cruz, CA 95064-1077, USA

Received 17 May 2002; accepted 18 February 2003

## Abstract

Thermistor chains and acoustic Doppler current profilers were deployed at the northern and southern ends of Monterey Bay to examine the thermal and hydrodynamic structure of the inner ( $h \sim 20$  m) shelf of central California. These instruments sampled temperature and current velocity at 2-min intervals over a 13-month period from June 2000 to July 2001. Time series of these data, in conjunction with SST imagery and CODAR sea surface current maps, helped to establish the basic hydrography for Monterey Bay. Analysis of time series data revealed that depth integrated flow at both sites was shore parallel (northwest–southeast) with net flows out of the Bay (northwest). The current and temperature records were dominated by semi-diurnal and diurnal tidal signals that lagged the surface tides by 3 h on average. Over the course of an internal tidal cycle these flows were asymmetric, with the flow during the flooding internal tide to the southeast typically lasting only one-third as long as the flow to the northwest during the ebbing internal tide. The transitions from ebb to flood were rapid and bore-like in nature; they were also marked by rapid increases in temperature and high shear. During the spring and summer, when thermal stratification was high, we observed almost 2000 high-frequency ( $T_p \sim 4\text{--}20$  min) internal waves in packets of 8–10 following the heads of these bore-like features. Previous studies along the West Coast of the US have concluded that warm water bores and high-frequency internal waves may play a significant role in the onshore transport of larvae.

Published by Elsevier Science Ltd.

*Keywords:* Inner shelf; Upwelling; Internal tides; Internal waves; Currents; Temperature

## 1. Introduction

During the past 20 years, a number of studies investigating the circulation of Monterey Bay and

the adjacent shelf have been conducted (Strub et al., 1987; Noble et al., 1992; Breaker and Broenkow, 1989; Breaker and Broenkow, 1994; Rosenfeld et al., 1994; Paduan and Rosenfeld, 1996; Rosenfeld et al., 1999; Xu et al., 2002). Remotely sensed and in situ data from these studies have provided a picture of the surface and internal circulation patterns on the middle and outer shelf. The circulation has been characterized

\*Corresponding author. Tel.: +1-831-427-4721; fax: +1-831-427-4728.

E-mail addresses: [dstorlazzi@usgs.gov](mailto:dstorlazzi@usgs.gov) (C.D. Storlazzi), [margaret@es.ucsc.edu](mailto:margaret@es.ucsc.edu) (M.A. McManus), [figurski@biology.ucsc.edu](mailto:figurski@biology.ucsc.edu) (J.D. Figurski).

by two end-members: a spring–summer regime and a fall–winter regime.

During the spring and summer, the winds are predominantly northwesterly due to a region of high-pressure offshore central California known as the California High. Persistent southeasterly winds result in the upwelling of cold, nutrient-rich bottom waters. Upwelling centers are often located at headlands where wind-stress curl is enhanced by orographic effects (Miller et al., 1999). The tongue of cold upwelled water that originates north of Monterey Bay is advected southward across the mouth of the Bay (Rosenfeld et al., 1994). At this

time the circulation inside Monterey Bay is characterized by a counter-clockwise surface eddy (Graham, 1993; Graham and Largier, 1997; Paduan and Rosenfeld, 1996). This eddy, with a residence time of 8–10 days, is typified by warmer surface waters (Fig. 1). During the winter the winds are more variable, often westerly to southwesterly due to a region of low pressure known as the Aleutian Low centered over the western Gulf of Alaska. This wintertime system drives storms across northern and central California (Strub et al., 1987). At this time, mean flows are characterized by alongshore (northwest) barotropic currents in

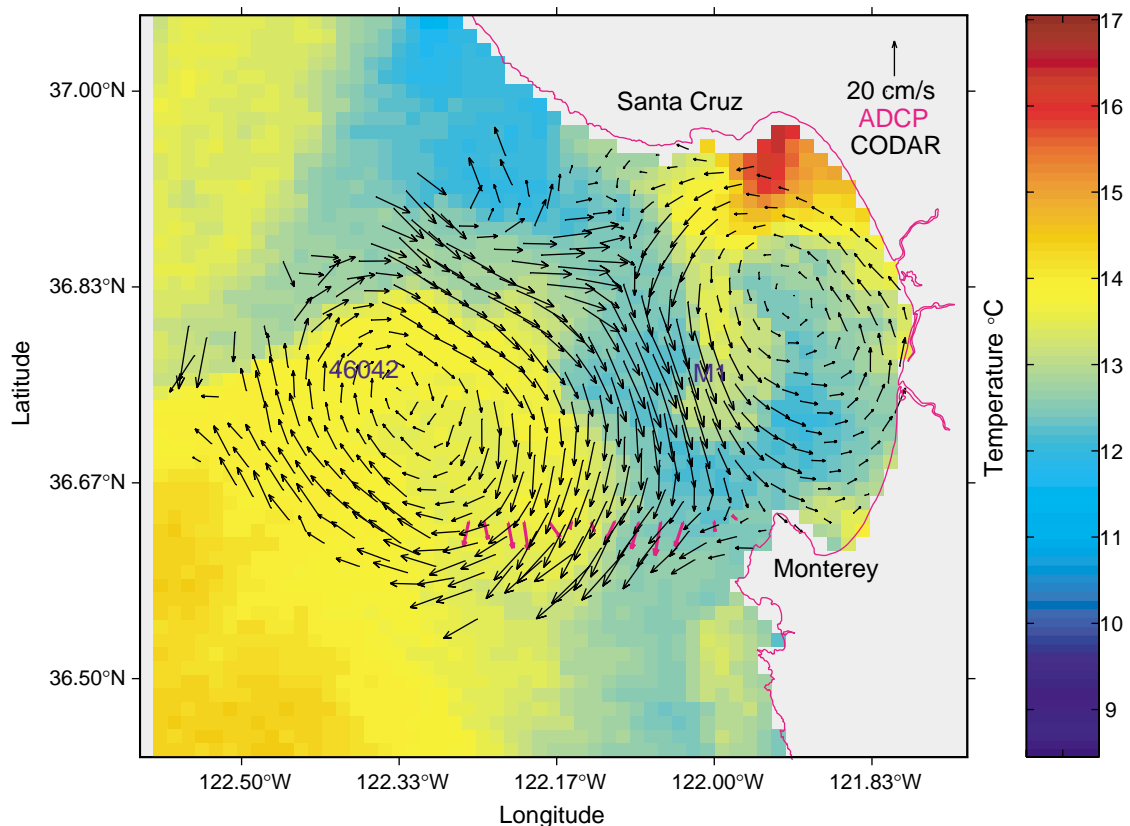


Fig. 1. Typical surface currents and SSTs for the Monterey Bay area during upwelling conditions in early August 1994. Average CODAR-derived surface currents (black) and average VM-ADCP near-surface current vectors (magenta) are overlaid on uncorrected AVHRR Channel 4 SSTs. Cool, deep water (blue) is upwelling along the coast and the warmer surface water (yellow, red) forced offshore. A tongue of cold water is detached from the shoreline just north of Monterey Bay and is being driven down the coast and into the bay by strong persistent winds to the southeast. A warm pool exists in the northeastern part of the bay and the surface current field exhibits the two typical circulation cells: an anti-cyclonic eddy offshore and an eddy with cyclonic motion in the bay. [Reproduced with permission from the American Geophysical Union, from Paduan and Rosenfeld (1996)].

addition to large, low-frequency baroclinic fluctuations (Strub et al., 1987).

In addition to studies investigating the larger-scale circulation of Monterey Bay and the adjacent shelf, there have been several studies investigating flow on the inner shelf ( $h < 20$  m) of Monterey Bay. These studies have primarily been benthic boundary layer sediment transport studies (Stanton, 2001; Storlazzi and Jaffe, 2002), investigating flow within a meter of the bed. Understanding the hydrodynamic nature of the relatively unexplored region of the inner shelf is crucial to understanding biological, chemical and geological exchanges between the shoreline and the adjacent shelf.

In this paper, we explore the structure and timing of cycles of currents and water temperature along the embayed inner shelf of central California based on acoustic Doppler current profiler (ADCP) and thermistor data from two locations in the region of Monterey Bay. Several aspects of the data will be discussed: First, we will describe the seasonal cycle of currents and temperature fluctuations at each of the sites so that the relative magnitudes and phases of these fluctuations at different locations can be compared. We will then relate these fluctuations to larger-scale oceanographic and atmospheric forcing. Another aspect we will address involves the high-frequency variations in the data records. Included in this will be the analysis of motions on the order of minutes to hours, which include high-frequency (4–20 min) internal waves and internal tidal motions (12.4–24.8 h).

## 2. Methods

Two upward-looking RD Instruments 600 kHz ADCPs were deployed nearly continuously in roughly 20 m of water off Sand Hill Bluff (SHB) and Hopkins Marine Station (HMS) in Monterey Bay from June 2000 to June 2001 (Fig. 2). The ADCPs were bolted via PVC frames to pipes jettied into the sandy sea floor; this made the ADCPs extremely stable. Measurements of current velocity in the  $x$ -,  $y$ - and  $z$ -axis along with acoustic backscatter intensity were made at 1 m intervals from 3 m above the bed up to the surface. The

ADCPs averaged 40 pings every 2 min (0.0083 Hz) providing observations of currents and backscatter at 20 different elevations above the bed. Time series of ADCP data were pre-processed by removing all data when the beam correlation dropped below 80%.

Approximately 15 m away from each ADCP was a thermistor chain, with one temperature sensor near the bed, one in mid-water column and one just below the surface ( $z \sim 1, 8, 16$  m, respectively). Each sensor sampled temperature on 2 min intervals. The ADCPs and thermistors were recovered, downloaded, refurbished, and redeployed generally once a month. Hourly wave height and period, wind speed and direction, and sea level barometric pressure data were obtained from the National Data Buoy Center's (NDBC) Monterey Buoy #46042 roughly 140 km west of Moss Landing in 2000 m of water. Hourly tidal elevation observations relative to mean sea level were recorded by the National Ocean Service at Monterey Harbor (CO-OPS, 2002). Select sea surface temperature (SST) maps of the region off-central California were collected by the NOAA-16 polar-orbiting satellite and downloaded from the CoastWatch West Coast Regional Node web page (<http://cwatchwc.ucsd.edu/cwatch.html>).

## 3. Results

### 3.1. Inter-seasonal variability

A 12-month time series of tidal height, mean daily wind vectors and mean daily current vectors from SHB and HMS are presented in Fig. 3. Daily depth-averaged currents at SHB are oriented parallel to shore (northwest–southeast) 99.7% of the time, with currents flowing out of the Bay (to the northwest) 89.2% of the time. Current variability was slightly higher at the HMS station, with the daily mean currents being shore parallel (northwest–southeast) 96.3% of the time, and out of the Bay (to the northwest) 77.8% of the time. Southeastward mean currents at both locations were observed only during neap tides. On average, daily depth-averaged currents at SHB were two–four times greater in magnitude than at HMS

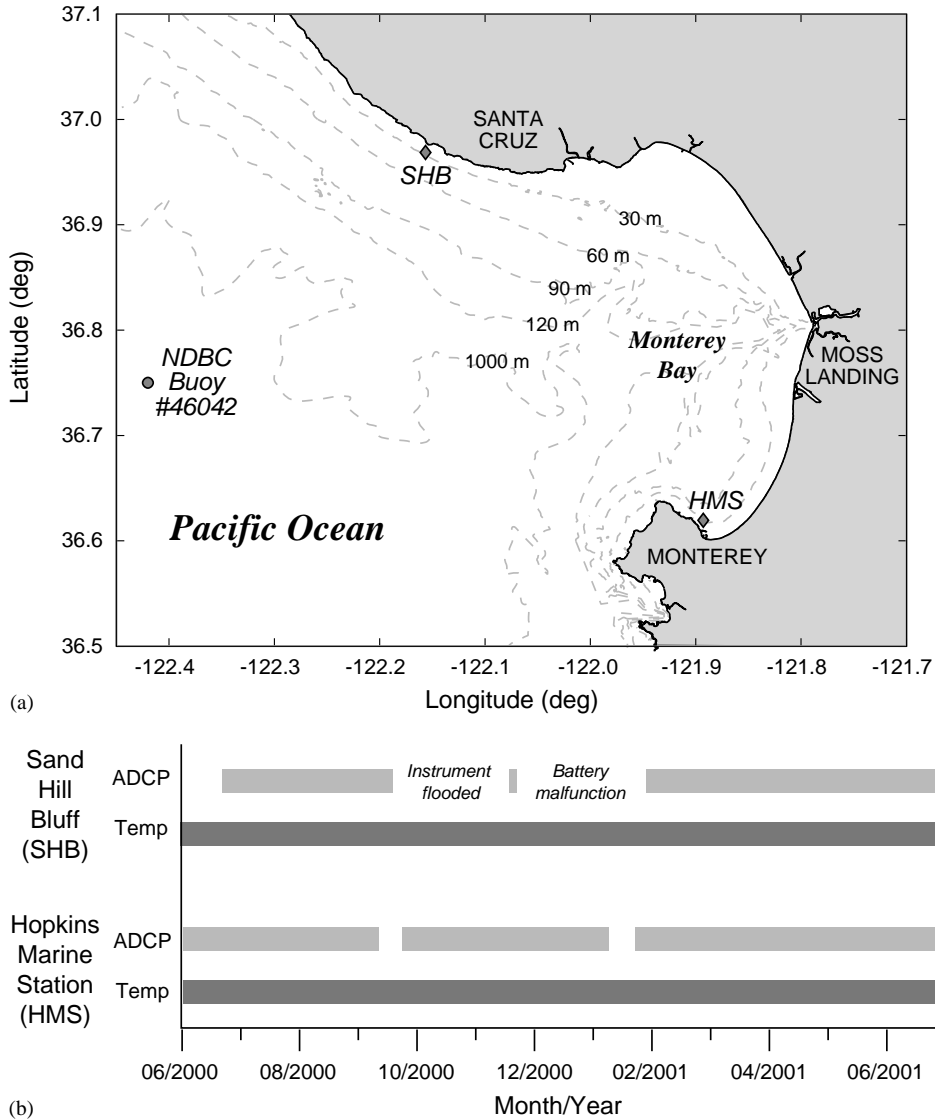
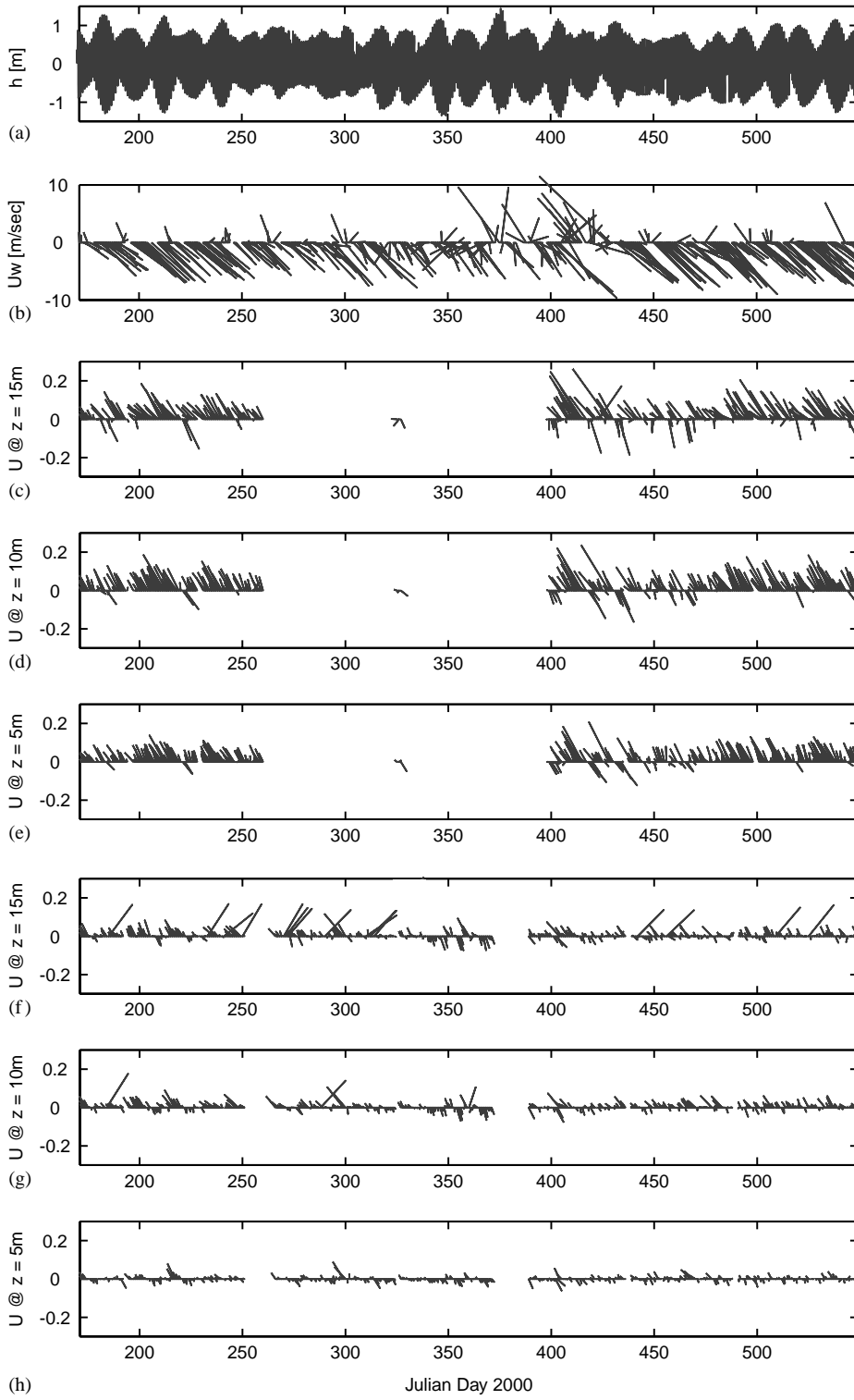


Fig. 2. Study area, instrument locations and data records discussed in this paper: (a) map of the study area showing the location (diamonds) of the ADCPs and thermistor chains and the NDBC's Monterey Buoy #46042; (b) timelines of instrument data recovery. The ADCPs and thermistors were recovered, downloaded, and refurbished every month. During the times of coverage, both the ADCPs and thermistors recorded data every 2 min.

(9 cm/s vs. 5 cm/s at  $z = 15$  m; 8 cm/s vs. 2 cm/s at  $z = 5$  m). However, shear was three times greater at HMS than at SHB, with shears averaging 0.035

and  $0.013 \text{ s}^{-1}$ , respectively (shear calculated between  $z = 5$  and 15 m after [Itsweire et al., 1989](#)). The daily depth-averaged current vectors (to the

Fig. 3. Time series of data from June 2000 to July 2001: (a) hourly tidal height (m) from NOS Monterey station; (b) mean daily wind speed (m/s) and direction ( $^\circ$ ) from the NDBC buoy; (c–e) SHB: mean daily current speed (m/s) and direction ( $^\circ$ ) at three depths above the bottom; and (f–h) HMS: mean daily current speed (m/s) and direction ( $^\circ$ ) at three depths above the bottom. All the vectors are shown in geographic orientation.



northwest) were not correlated with near-surface currents (to the southeast) measured by both the upward-looking ADCP (upper bins not shown) and CODAR (<http://www.oc.nps.navy.mil/~radlab/radar.html>). Nor is there a correlation between daily depth-averaged current vectors and daily averaged wind vectors observed at the NDBC buoy at either site. Similar trends were noted by Paduan and Rosenfeld (1996).

The energy in the near-surface and near-bed alongshore currents at SHB and HMS is dominated by the diurnal and semi-diurnal tidal signals at 0.04 and 0.08 cycles/h, respectively (Figs. 4 and 5). At SHB, the cross-shore current spectra are similar to the alongshore currents spectra but they display a slightly higher variance across all bands. The energy in the cross-shore currents at HMS, however, is dominated by high-frequency fluctuations. Possible explanations for this difference between cross-shore flow at the two sites will be addressed later. There are very small, statistically insignificant peaks in energy variance at both the diurnal and semi-diurnal tidal frequencies.

The near-surface backscatter spectra at SHB and HMS show high energy in the diurnal and semi-diurnal tidal frequencies. In contrast to the current spectra, the near-surface and near-bed backscatter display significantly higher-energy variance at both higher and lower frequencies. This pattern is likely related to periods when high-frequency internal wave packets or large winter storm waves suspend large quantities of bottom sediment up to  $z > 12$  m above the bed.

The temperature spectra at both sites are dominated by diurnal and semi-diurnal tidal frequencies but show substantially more energy at lower frequencies ( $> 24$  h) than the alongshore current spectra. This is most likely a reflection of upwelling/relaxation cycles and inter-seasonal variability. These spectra also show relatively small contributions by higher-frequency motions likely related to high-frequency internal wave packets.

### 3.2. Seasonal variability

#### 3.2.1. June 23–August 2 (Julian Day 175–215)

The spring–summer regime is characterized by strong persistent winds out of the northwest

(Fig. 6) resulting from the California High positioned off the West Coast of the US. As discussed previously, current magnitudes are higher at SHB than HMS. In addition, HMS shows warmer overall temperatures than those observed at SHB, and typically displays a much greater temperature difference across the water column. As seen in the power spectra, semi-diurnal alongshore currents dominate the flow at both sites. Semi-diurnal fluctuations in temperature, on the order of 2–4°C, are also evident in the time series. There is a strong correlation between the semi-diurnal tide and the temperature fluctuations at both SHB and HMS. At SHB, flows out of the Bay (to the northwest) coincide with warming, while flows into the Bay (to the southeast) coincide with cooling. At HMS, the coupling between temperature and currents is reversed, flows out of the Bay (to the northwest) coincide with cooling, while flows into the Bay (to the southeast) coincide with warming.

Although winds are predominantly from the northwest during the spring and summer, there are periods where winds decrease substantially or reverse direction. These periods are termed “relaxation events”. The water column is observed to warm in response to these relaxation events. These low-frequency warming events are superimposed on the high-frequency semi-diurnal temperature oscillations discussed previously. Warming in response to relaxation events are evident throughout the summer, the most significant events occurring from 28 June to 3 July (Julian Day 180–185) and from 10 to 13 July (Julian Day 192–195). The lag between relaxation-favorable winds and the maximum water column warming is typically less at SHB (0–1 day) than at HMS (1–2 days).

#### 3.2.2. January 29–March 10 (Julian Day 395–435)

Higher-velocity winds from the southeast, and larger waves characterize the winter period shown in Fig. 7 as strong storms track across the North Pacific Ocean. During the winter months, the California High is replaced by the Aleutian Low. The result: storm systems take on a more southern track across the West Coast of the US, causing more frequent periods of winds and waves propagating to the east or northeast. During the

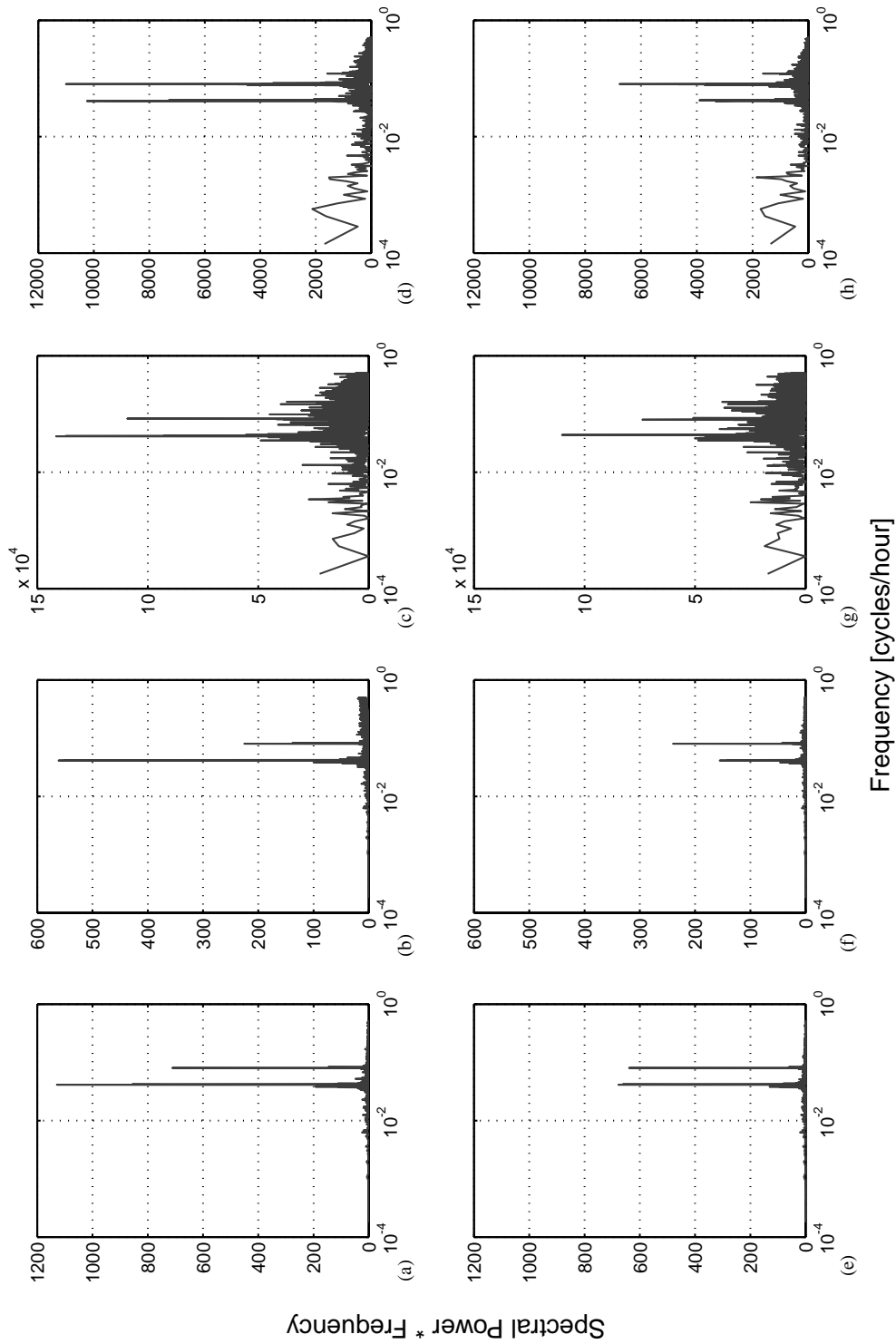


Fig. 4. Variance-conserving power spectra of the oceanographic data from the SHB study site: (a) hourly alongshore currents at  $z = 5$  m; (b) hourly cross-shore currents at  $z = 5$  m; (c) hourly acoustic backscatter  $z = 5$  m; (d) hourly temperature from the top thermistor; (e) hourly alongshore currents at  $z = 15$  m; (f) hourly cross-shore currents at  $z = 15$  m; (g) hourly acoustic backscatter  $z = 15$  m; and (h) hourly temperature from the bottom thermistor. Note the varying scales on the y-axis.

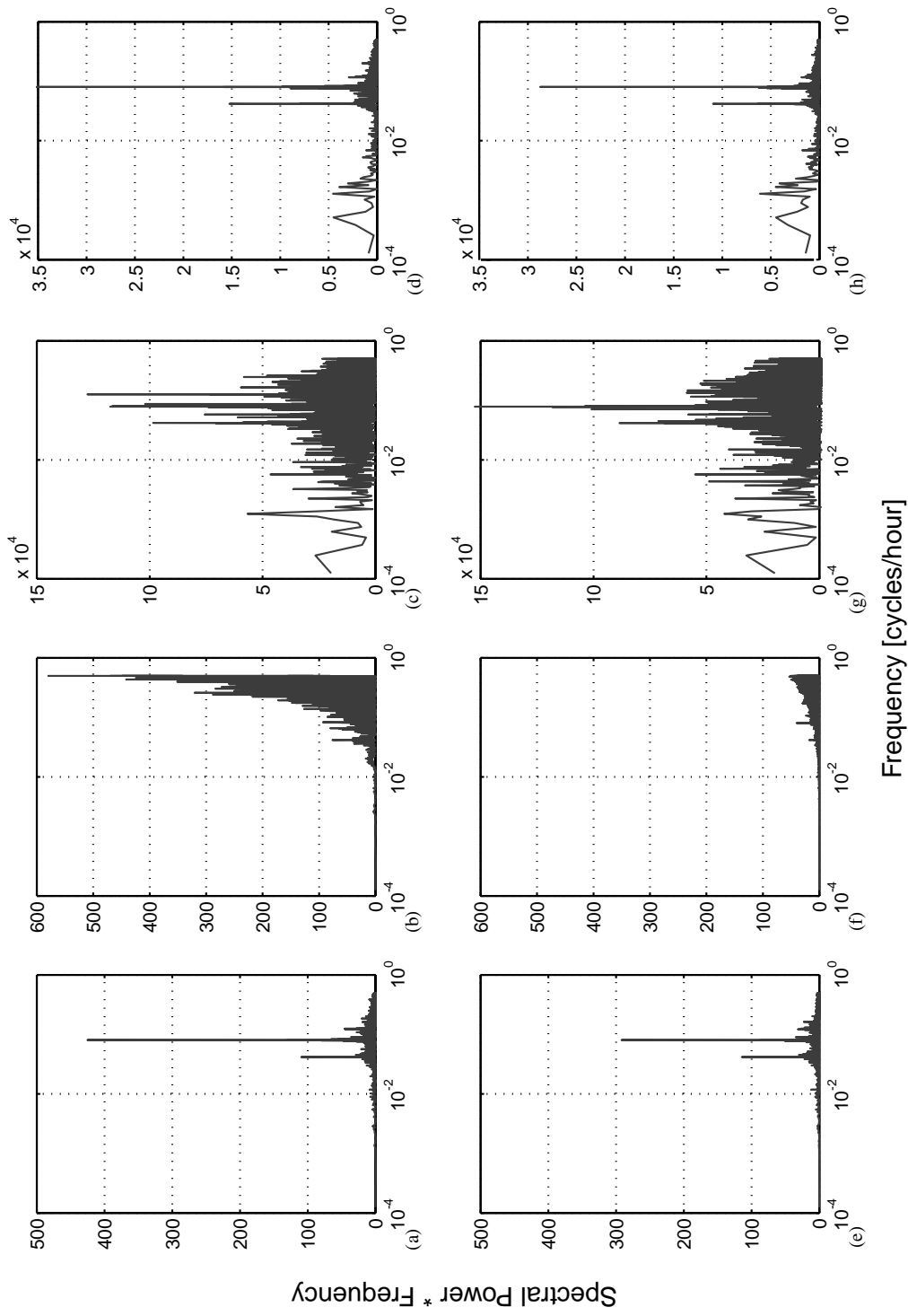


Fig. 5. Variance-conserving power spectra of the oceanographic data from the HMS study site: (a) hourly alongshore currents at  $z = 5$  m; (b) hourly cross-shore currents at  $z = 5$  m; (c) hourly acoustic backscatter  $z = 5$  m; (d) hourly temperature from the top thermistor; (e) hourly alongshore currents at  $z = 15$  m; (f) hourly cross-shore currents at  $z = 15$  m; (g) hourly acoustic backscatter  $z = 15$  m; and (h) hourly temperature from the bottom thermistor. Note the varying scales on the y-axis.

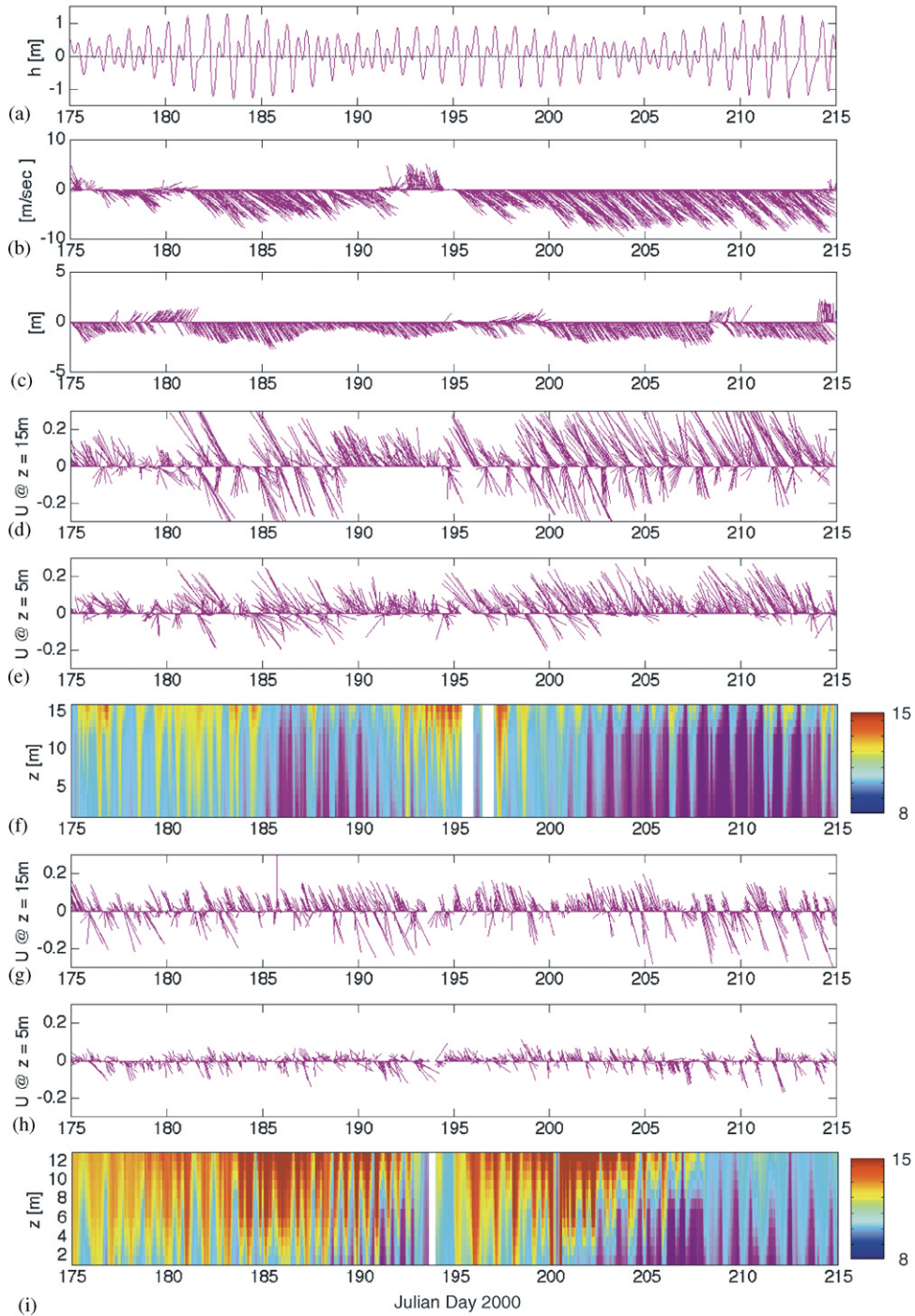


Fig. 6. Time series of hourly mean data from 23 June to 2 August 2000: (a) tidal height (m); (b) wind speed (m/s) and direction ( $^{\circ}$ ); (c) wave height (m) and direction ( $^{\circ}$ ); (d) SHB: current velocities (m/s) at  $z = 15$  m; (e) SHB: current velocities (m/s) at  $z = 5$  m; (f) SHB: water temperature ( $^{\circ}$ C); (g) HMS: current velocities (m/s) at  $z = 15$  m; (h) HMS: current velocities (m/s) at  $z = 5$  m; and (i) HMS: water temperature ( $^{\circ}$ C).

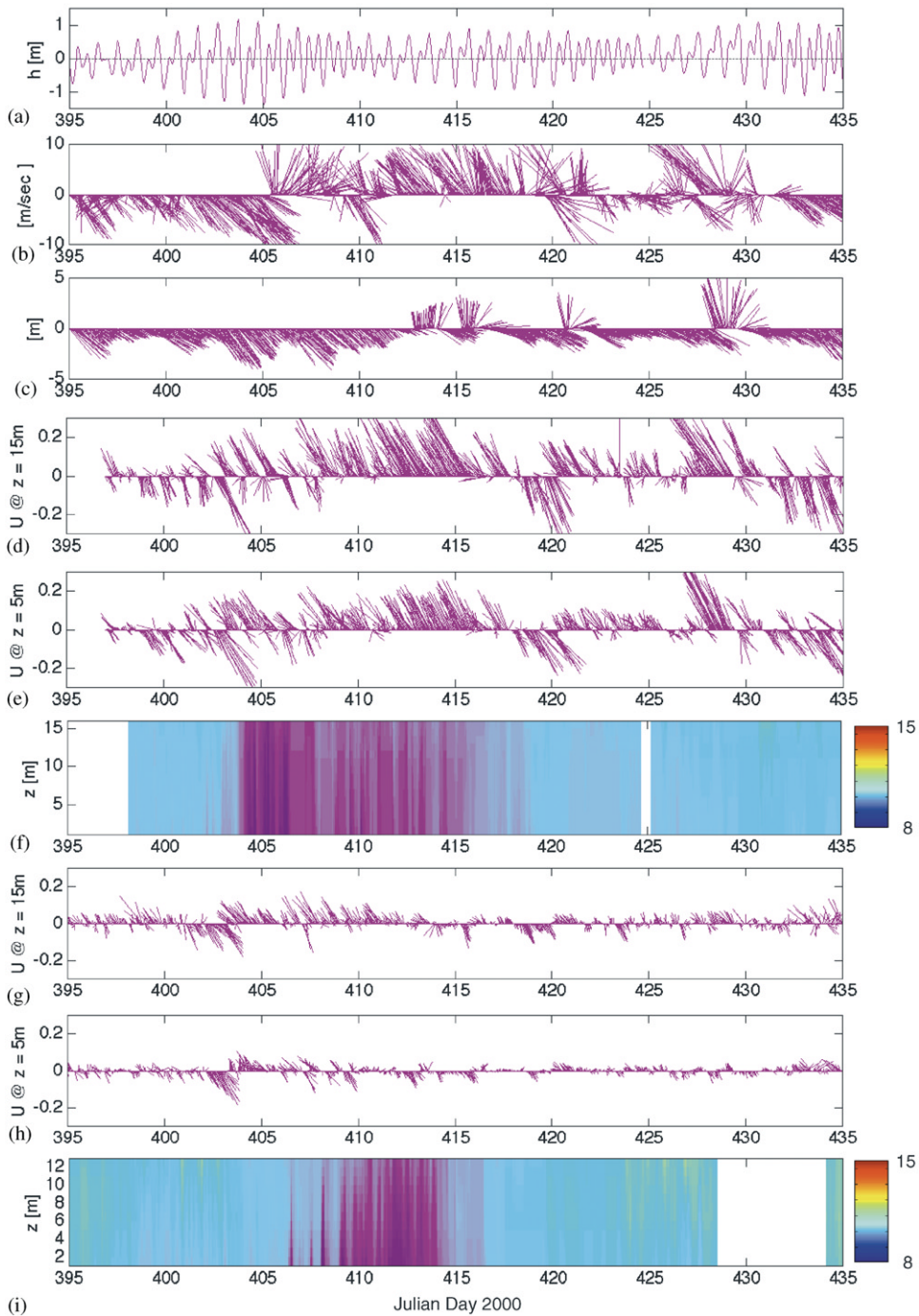


Fig. 7. Time series of hourly mean data from 29 January to 10 March 2001: (a) tidal height (m); (b) wind speed (m/s) and direction ( $^{\circ}$ ); (c) wave height (m) and direction ( $^{\circ}$ ); (d) SHB: current velocities (m/s) at  $z = 15$  m; (e) SHB: current velocities (m/s) at  $z = 5$  m; (f) SHB: water temperature ( $^{\circ}$ C); (g) HMS: current velocities (m/s) at  $z = 15$  m; (h) HMS: current velocities (m/s) at  $z = 5$  m; and (i) HMS: water temperature ( $^{\circ}$ C).

winter months, the water column is well mixed, temperatures are cooler and almost uniform from the surface to the bottom. With the exception of storm periods, the mean hourly current speeds are lower than during the spring and summer (Fig. 6). Higher mean current velocities during spring tides and the semi-diurnal current reversals are again evident but are strongly overprinted by sustained unidirectional full-water column net flow to the northwest during the passage of storms.

### 3.3. *Internal tidal motions*

A 3 day time series of tidal height, current velocity, acoustic backscatter and temperature from HMS is shown in Fig. 8. Although the current speeds during this time are predominantly diurnal, a 12.4 h semi-diurnal signal is also apparent; the backscatter and temperature records are dominated by a semi-diurnal signal. As discussed previously, mean alongshore current velocities are higher than the mean cross-shore current velocities. During the ebb tide, the depth-averaged currents flow out of the Bay (to the northwest), increasing to peak velocity just before low water. During the ebb tide there was significant shear ( $\sim 0.13 \text{ s}^{-1}$ ) in the water column, with the near-bed flow ( $z < 4 \text{ m}$ ) into the Bay (to the southeast) at roughly 5 cm/s, with the rest of the flow in the water column out of the Bay (to the northwest) at more than 5 cm/s. Acoustic backscatter in the water column increased gradually during the ebb tide, and water temperatures were observed to cool. Overall, the ebb tides are typically 3–3.5 times longer than periods of flood tide.

Following the ebb tide, the depth-averaged currents reverse abruptly and flood into the Bay (to the southeast). At these sharp transitions from ebb to flood tide, the total backscatter decreases and temperature increases by over  $4^\circ\text{C}$  through most of the water column (Fig. 9). The asymmetrical nature and semi-diurnal pattern of internal motions seen in both the ADCP and thermistor data suggests that these motions are likely internal tidal bores. Vertical velocities, which are typically within the error of the sensors ( $\pm 2 \text{ cm/s}$ ), rapidly fluctuate  $\pm 5 \text{ cm/s}$  throughout much of the water column following internal tidal bores. Temperatures also display similar high-frequency fluctua-

tions (internal waves) following the transitions. The temporal and vertical structure of warm water internal tidal bores propagating into the Bay followed by high-frequency internal waves are very similar to the observations made by Pineda (1994a, b, 1996) off Southern California. Net near-bed flow during the passage of these high-frequency internal waves was oriented offshore while net flow higher up in the water column was oriented onshore. These observations have consequences for the ability of these types of internal waves to transport material higher up in the water column such as larvae onshore similar to the observations of Pineda (1994a, b, 1996), while sea floor sediment suspended by the internal waves' motions would be advected offshore. It should be noted that the internal tides lag the surface tides by roughly 3 h on average, a similar trend was observed by Petrucio et al. (1997) in the Monterey Submarine Canyon.

### 3.4. *High-frequency internal waves*

The temperature time series was searched for internal waves using an automated algorithm that identified oscillations (wave-like fluctuations) greater than  $0.5^\circ\text{C}$  with periods between 2 and 24 min. Seven hundred and fifty individual internal waves were observed at the SHB and 1220 individual internal waves were observed at HMS. A majority of the waves were observed in “packets” or “trains” of 6–19 waves per packet, with an average of  $10.3 \pm 4.1$  individual waves per packet at SHB and  $8.4 \pm 1.2$  individual waves per packet at HMS. The mean intensity, period, and speed of internal waves per packet are shown in Fig. 10. The mean temperature oscillations and wave propagation speeds per internal wave packet were slightly lower at the SHB site ( $0.8 \pm 0.7^\circ\text{C}$  and  $12 \pm 2 \text{ cm/s}$ ) than at the HMS site ( $0.9 \pm 0.7^\circ\text{C}$  and  $13 \pm 2 \text{ cm/s}$ ), while the mean wave period per packet were longer at SHB than at HMS ( $11.3 \pm 9.9 \text{ min}$  vs.  $9.7 \pm 9.1 \text{ min}$ ). The internal wave packets typically occurred when the thermal stratification was  $1.1 \pm 0.5^\circ\text{C}$  at SHB and  $2.0 \pm 1.4^\circ\text{C}$  at HMS. The minimum thermal stratification measured when any internal waves were observed at either site was  $0.4^\circ\text{C}$ , while more than 90% of the internal waves were observed

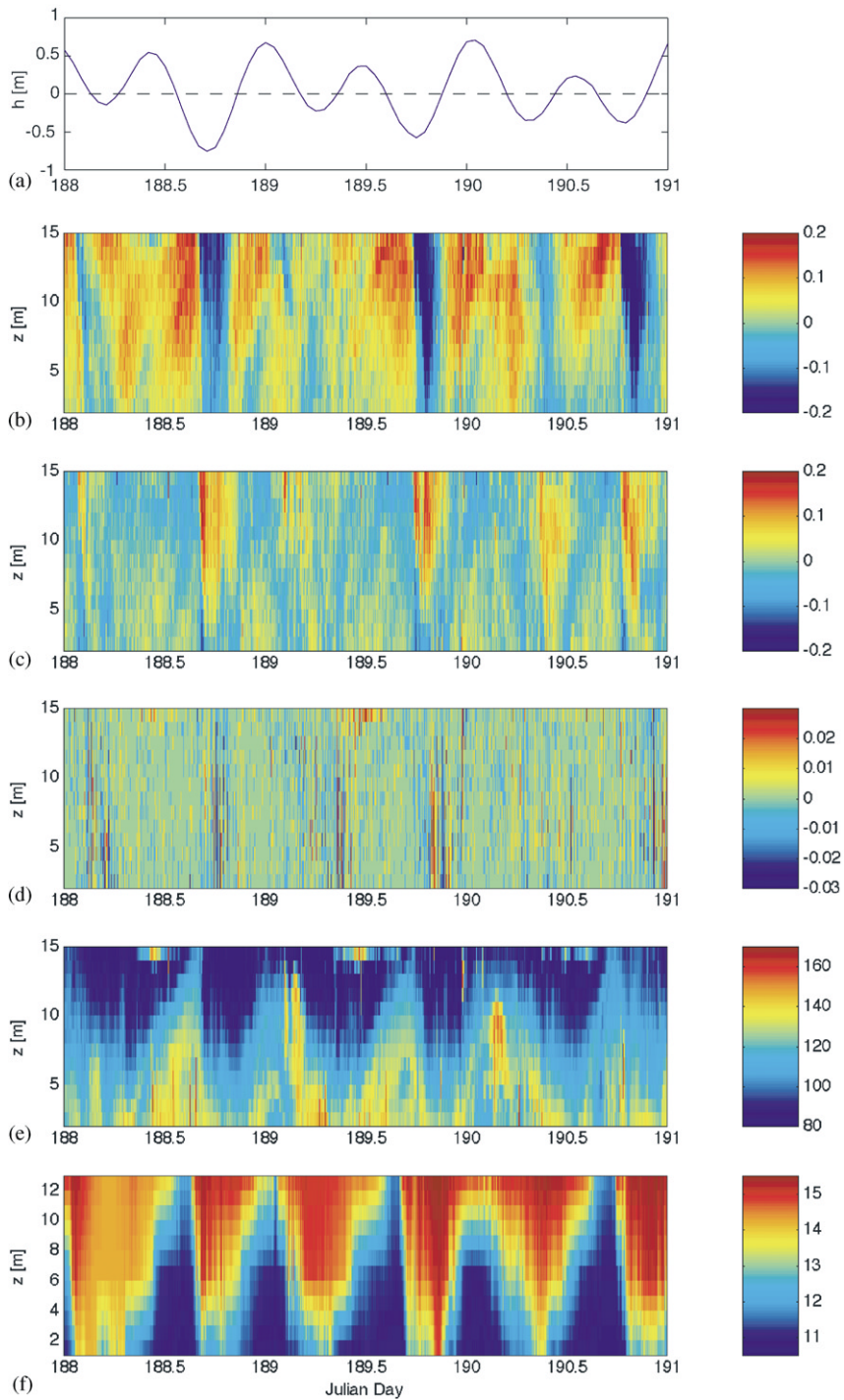


Fig. 8. Data displaying the asymmetric nature of the internal tides at the HMS site and the lag between the surface tides and the internal tides: (a) tidal height (m); (b) alongshore (to the northwest) current velocities (m/s); (c) onshore current velocities (m/s); (d) upward current velocities (m/s); (e) acoustic backscatter intensity (dB); and (f) water temperature ( $^{\circ}\text{C}$ ). The tidal data were collected hourly, the current and temperature data were collected every 2 min.

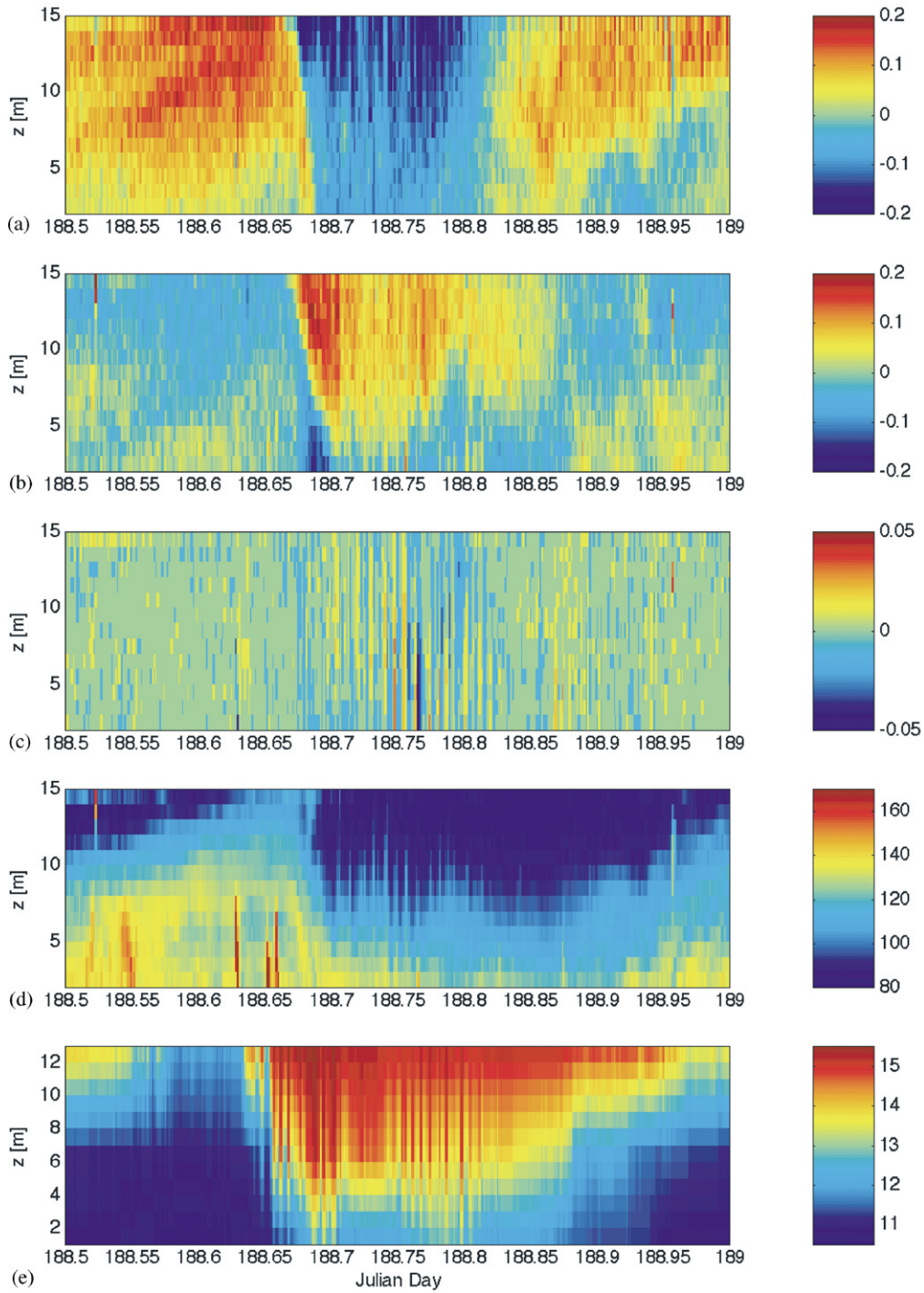
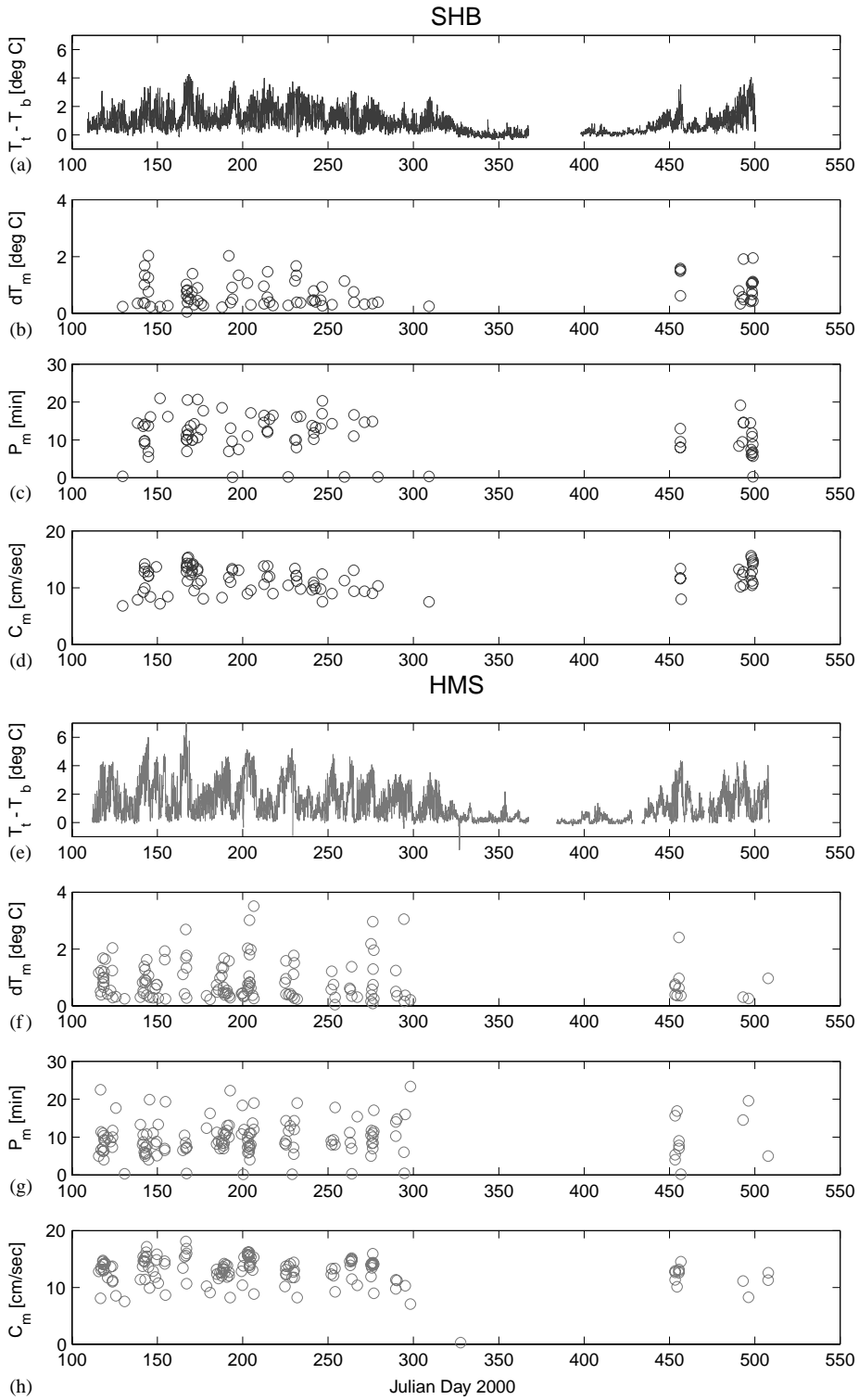


Fig. 9. Temporal structure of an asymmetric internal tidal bore and the associated high-frequency internal waves following the head of the bore at the HMS site: (a) alongshore (to the northwest) current velocities (m/s); (b) onshore current velocities (m/s); (c) upward current velocities (m/s); (d) acoustic backscatter intensity (dB); and (e) water temperature (°C).



when the stratification was greater than  $0.7^{\circ}\text{C}$  and  $0.6^{\circ}\text{C}$  at the SHB and HMS sites, respectively.

The internal waves' occurrence appeared to be linked to the lunar monthly cycle, with them being observed between the spring and neap tides. The maximum and minimum tidal ranges over the deployment period were 2.2 and 1.3 m, respectively (CO-OPS, 2002). All of the more than 1900 internal waves observed at both sites occurred when the tidal range was between the relatively narrow limits of 1.5 and 1.7 m. Observations of physical structure and shear in Monterey Bay show that during spring tides shear is high; however, tidal mixing causes the water column to destratify. Thus, there is no density interface to support internal wave activity. During neap tides the water column is stratified, however shear is low. Thus there is no generating mechanism for internal waves. The roughly 150 days during the winter in which no high-frequency internal waves were observed (Julian Day 310–460) is likely due to the breakdown in thermal stratification observed in Fig. 7. This lack of stratification is likely due to the strong mixing by large winter waves, decreased insolation during central California's rainy winter and the much more variable and thus less upwelling-favorable wind field due to the passage of storms.

#### 4. Discussion

##### 4.1. Spring–summer upwelling/relaxation and winter storms: implications for the inner shelf

While the impacts of upwelling and relaxation events on SST along the West Coast of the US have been known for many years, there has been little documentation on how these regional processes contribute to internal fluid motions and thermal variability on the inner shelf. When the

warm water mass that is kept offshore by wind-driven Eckman transport during upwelling periods is advected onshore as the winds diminish or reverse to the northwest, the entire water column warms on a magnitude similar to the SSTs ( $2\text{--}5^{\circ}\text{C}$ ) and stratification completely breaks down. While SSTs typically stay high for a few days after the onset of a relaxation event, it appears that the diurnal to semi-diurnal internal tidal motions quickly ( $<24\text{h}$ ) mix and/or replace the warm bottom water with cooler water, causing an increase in stratification. In the absence of other processes, thermal stratification is greater during neap tides when the current speeds, and thus shear and turbulent mixing, are lower.

As winter storms impact Central California, we see a concurrent breakdown in stratification, which is likely due to the increased wave-induced mixing in the water column. SSTs drop due to decreased insolation; however, near-bed water temperatures, while cool, are not substantially different from those observed during periods of strong upwelling. The winter storms that commonly track farther south and directly strike California have interesting implications on the study area. When the winter storms strike the central coast, they are typically preceded by southwesterly winds that mix to 20+ m and intensify depth-averaged flow to the northwest, especially at the SHB site. These winds appear to drive surface water onshore causing water to “pond” up along the shoreline (Storlazzi and Griggs, 2000) as shown by the super-elevated tides during the periods of February 15–20 (Julian Day 412–417) and March 1–5 (Julian Day 426–430) when tidal heights are up to 10 s of cm above mean sea level (cf. Fig. 7). The effects of this “ponding”, which is intensified in the many south-facing log-spiral bays along California due to their orientation relative to the storm tracks, can be seen in the SHB site's current records periods after the

Fig. 10. Temporal variation in thermal stratification and the high-frequency internal wave's structure at both sites during the study: (a) SHB: Difference in temperature between the top and bottom thermistor ( $^{\circ}\text{C}$ ); (b) SHB: Mean amplitude of temperature change induced by internal waves per packet ( $^{\circ}\text{C}$ ); (c) SHB: Mean internal wave period per packet (min); (d) SHB: Mean internal wave propagation speed (m/s); (e) HMS: Difference in temperature between the top and bottom thermistor ( $^{\circ}\text{C}$ ); (f) HMS: Mean amplitude of temperature change induced by internal waves per packet ( $^{\circ}\text{C}$ ); (g) HMS: Mean internal wave period per packet (min); and (h) HMS: Mean internal wave propagation speed (cm/s).

passage of the storms. Following the storms of February 15–20 (Julian Day 412–417) and March 1–5 (Julian Day 426–429) there are high-velocity ( $\sim 30$  cm/s), sustained, depth-averaged flows to the southeast (Julian Day 418–420 and 430–431, respectively) that are not associated with north-westerly winds. These flows to the southeast are like due to pressure gradient forces after the release of the super-elevated water along the shoreline as the winds diminish or shift towards the southeast.

#### 4.2. Inner-shelf internal motions within the context of Monterey Bay circulation

During the flood tide, net cumulative flow measured over the course of a month was to the southeast at SHB and characterized by colder water, while at HMS the net flow was also to the southeast but characterized by warm water (Fig. 11a). Conversely, during the ebb tide, net flow over the course of a month was to the northwest at SHB characterized by warm water, while at HMS the net flow was also to the northwest but characterized by cool water.

During the flood tide at SHB, upwelled water is advected into the Bay, similar to the upwelling tongue observed in SST data (Fig. 1) and discussed by Rosenfeld et al. (1994). During the flood tide at HMS warm water is advected into the Bay, implying that some of the warm water pushed offshore by Eckman transport may be advected past HMS at flood tide. This signal also implies that the cold upwelled water observed to the north (i.e., at SHB and in the SST imagery) may be advected to the east of HMS. This may explain the cold water moving offshore during the ebbing tide at HMS. The cold water tongue may intersect the coastline somewhere between Monterey and Moss Landing where it then bifurcates, with one portion heading north into the counter-clockwise gyre typically observed in the CODAR and AVHRR SST images (Paduan and Rosenfeld, 1996), while the other portion flows south along the coastline. This portion of the cold water tongue would then hit the southern shoreline of the bay near Monterey Harbor and be advected to the northwest during the ebbing tide.

## 5. Summary

We utilized thermistor chains and ADCPs to examine the thermal and hydrodynamic structure of the inner ( $h \sim 20$  m) shelf of Monterey Bay, California. Time series of these data were analyzed in conjunction with SST imagery and CODAR sea surface current maps which provided a context of large-scale circulation. The ability to measure physical processes at high sampling rates ( $\sim 2$  min) over long time periods ( $\sim 12$  months) allowed us to investigate inner-shelf hydrography varying from high-frequency ( $T_p \sim 4$ – $20$  min) internal waves, to internal tides, to seasonal changes in physical hydrography. Critical findings from this analysis include:

- (1) Subsurface current velocities at both sites were shore parallel and out of the Bay (to the northwest), roughly opposite of the wind-driven surface flow.
- (2) Current and temperature records are dominated by semi-diurnal and diurnal internal tidal signals that lag the surface tides by roughly 3 h on average. These flows over the course of an internal tidal cycle are very asymmetric, with the flow during the flooding internal tide to the southeast typically lasting only one-third as long as the flow during the ebbing internal tide to the northwest.
- (3) The transitions of the internal tide from ebb to flood cycle are very rapid and bore-like in nature; they are also typically marked by rapid increases in temperature and high shear.
- (4) During the spring and summer when thermal stratification was high, almost 2000 high-frequency ( $T_p \sim 4$ – $20$  min) internal waves in packets of 8–10 were observed and typically followed the heads of these bore-like features.

## Acknowledgements

This research was made possible through funding from the Packard Foundation as part of the larger Partnership for Inter-disciplinary Studies of the Coastal Oceans (PISCO) Project. Dr. P. Raimondi and Dr. M. Carr directed the PISCO

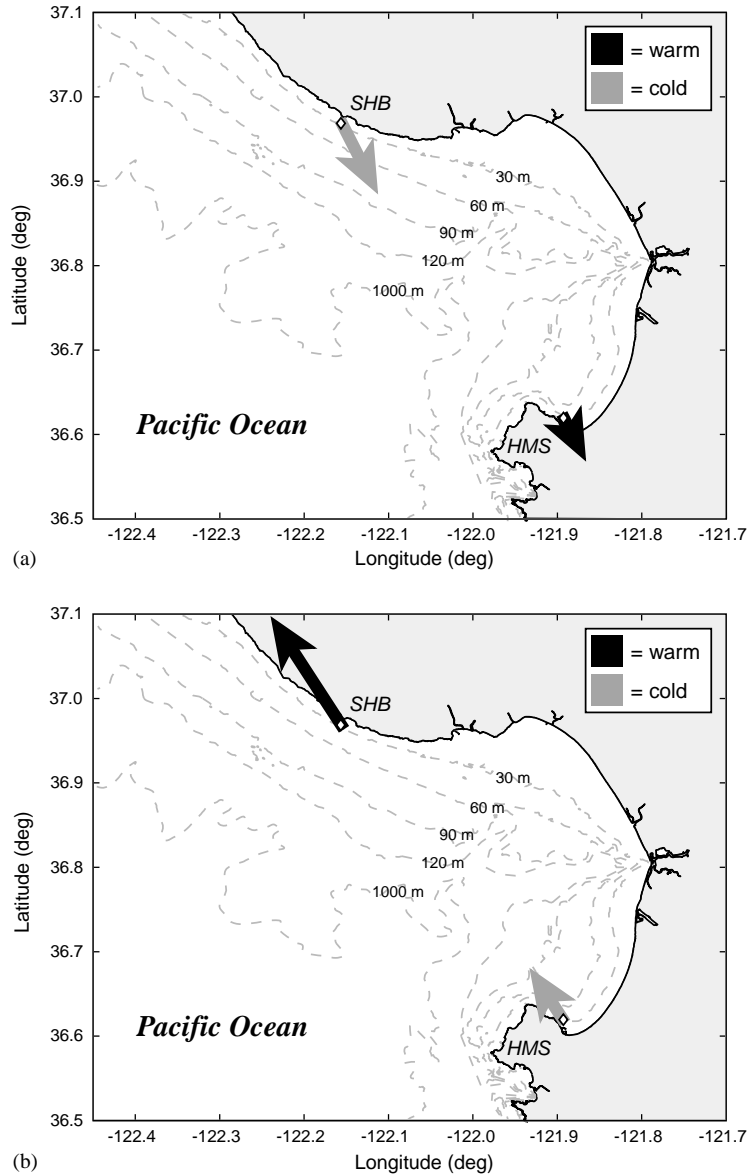


Fig. 11. Schematic diagram of the internal tides' depth-averaged flow magnitude, flow direction and relative temperature at both sites: (a) flooding internal tide; and (b) ebbing internal tide. The shade of the arrow denotes the water mass's relative temperature while the vector's length denotes its relative velocity. Average based on 12 months of data.

Project at the University of California, Santa Cruz and provided invaluable leadership and support. J. Grover and the other mooring technicians deserve special thanks for all the time and effort they contributed by running the instrument deployment, recovery, and refurbishment operations—

none of this work could have been completed without their long, hard work. We would also like to extend thanks to C. Cudaback (UCSB), J. Paduan (NPS) and L. Rosenfeld (NPS) for their substantial insight, cooperation, and critical review that contributed substantially to the goals of

this project. K. Donahue took care of all the little things that made everything run so much smoother, and for that we would like to thank her. We would like to thank Jingping Xu (USGS) and Holly Ryan (USGS) who provided constructive initial reviews of this manuscript. Steven Bograd and an anonymous reviewer for *Continental Shelf Research* also provided insightful reviews that contributed to this manuscript.

## References

- Breaker, L.C., Broenkow, W.W., 1989. The circulation of Monterey Bay and related processes. Technical Publication 89–1, Moss Landing Marine Laboratories, California, p. 91.
- Breaker, L.C., Broenkow, W.W., 1994. The circulation of Monterey Bay and related processes. *Oceanography and Marine Biology: An Annual Review* 32, 1–64.
- CO-OPS, 2002. Center for Operational Oceanographic Products and Services, National Ocean Service, National Oceanic and Atmospheric Administration. Electronic data, <http://co-ops.nos.noaa.gov/>.
- Graham, W.M., 1993. Spatio-temporal scale assessment of an “upwelling shadow” in northern Monterey Bay, California. *Estuaries* 16, 83–91.
- Graham, W.M., Largier, J.L., 1997. Upwelling shadows as nearshore retention sites: the example of Northern Monterey Bay. *Continental Shelf Research* 17 (5), 509–532.
- Itsweire, E.C., Osborn, T.R., Stanton, T.P., 1989. Horizontal distribution and characteristics of shear layers in the seasonal thermocline. *Journal of Physical Oceanography* 19, 301–320.
- Miller, A.J., McWilliams, J.C., Schneider, N., Allen, J.S., Barth, J.A., Beardsley, R.C., Chavez, F.P., Chereskin, T.K., Edwards, C.A., Haney, R.L., Kelly, K.A., Kindle, J.C., Ly, L.N., Moisan, J.R., Noble, M.A., Niiler, P.P., Oey, L.Y., Schwing, F.B., Shearman, R.K., Swenson, M.S., 1999. Observing and modeling the California Current System. *Eos, Transactions of the American Geophysical Union* 80 (45), 533–539.
- Noble, M.A., Ramp, S.R., Kinoshita, K., 1992. Current patterns over the shelf and slope adjacent to the Gulf of the Farallons, Executive Summary. USGS Open-File Report 92-382, p. 26.
- Paduan, J.D., Rosenfeld, L.K., 1996. Remotely sensed surface currents in Monterey Bay from shore-based HF radar (Coastal Ocean Dynamics Application Radar). *Journal of Geophysical Research* 101, 20669–20686.
- Petruncio, E.T., Rosenfeld, L.K., Paduan, J.D., 1997. Observation of the internal tide of Monterey. *Journal of Oceanography* 28, 1873–1903.
- Pineda, J., 1994a. Internal tidal bores in the nearshore: warm water fronts, seaward gravity currents and the onshore transport of neustonic larvae. *Journal of Marine Research* 52, 427–458.
- Pineda, J., 1994b. Circulation and larval distribution in internal tidal bore warm fronts. *Limnology and Oceanography* 44 (6), 1400–1414.
- Pineda, J., 1996. Internal tidal bore regime at nearshore stations along western USA: predictable upwelling within the lunar cycle. *Continental Shelf Research* 15, 1023–1041.
- Rosenfeld, L.K., Schwing, F.B., Garfield, N., Tracey, D.E., 1994. Bifurcated flow from an upwelling center: a cold water source for Monterey Bay. *Continental Shelf Research* 14 (9), 931–964.
- Rosenfeld, L.K., Paduan, J.D., Petruncio, E.T., Goncalves, J.E., 1999. Numerical simulations and observations of the internal tide in a submarine canyon. Proceedings of the ‘Aha Huliko’a Hawaiian Winter Workshop, University of Hawaii at Manoa, January 19–22, p. 8.
- Stanton, T.P., 2001. Monterey Inner Shelf Observatory (MISO). Electronic data, <http://www.oc.nps.navy.mil/~stanton/miso/misohome.html>.
- Storlazzi, C.D., Griggs, G.B., 2000. The influence of El Niño–Southern Oscillation (ENSO) events on the evolution of central California’s shoreline. *Geological Society of America Bulletin* 112 (2), 236–249.
- Storlazzi, C.D., Jaffe, B.E., 2002. Flow and sediment suspension events on the inner shelf of central California. *Marine Geology* 181, 195–213.
- Strub, P.T., Allen, J.S., Huyer, A., Smith, R.L., 1987. Seasonal cycles of currents, temperatures, winds, and sea level over the northeastern Pacific continental shelf: 35 deg N–48 deg N. *Journal of Geophysical Research* 92, 1057–1062.
- Xu, J.P., Noble, M.A., Eittem, S.L., 2002. Suspended sediment transport on the continental shelf near Davenport, California. *Marine Geology* 181, 171–194.